PROC. OF JSCE
No. 318, February 1982

FINITE DIFFERENCE ANALYSIS OF REINFORCED CONCRETE PLATE WITH MATERIAL NONLINEARITY

By Lie-Liung CHOU, Masahiro KAWAGUCHI** and Tada-aki TANABE****

1. INTRODUCTION

Studies of the response of the reinforced concrete slabs to static loads have been done in the past. Because of the complexities involved, however, no simple analytical approach has been developed. Some of the complexities are enumerated below:

(1) The structural system is three-dimensional and is composed of two different materials, concrete and steel.
(2) The structural system has a continually changing character due to the cracking of the concrete under increasing load.
(3) The effects of (a) the dowel action in the steel reinforcement, (b) bond between the reinforcement and the concrete and (c) bond slip are difficult to be incorporated into a general analytical model.
(4) The stress-strain relationship for the concrete is nonlinear and is a function of many variables.

In view of such great complexities, an analysis to determine principal stresses throughout reinforced concrete members by classical theories is virtually impossible.

Recently the finite element method has been used for the investigation of nonlinear behavior of reinforced concrete structures. Ngo and Scordelis[16], C. H. Nam and C. G. Salmon[8] studied simple beam problems. J. C. Jofriet and G. M. McNeice[13] studied the behavior of simple beams and corner supported two-way slab. M. K. Wanchoo and G. W. May[14] studied the cracking behavior of reinforced concrete plates. Their analytical results were acceptable but not fully successful because of the complexities involved in establishing a suitable finite element approach that could utilize a proper constitutive law for reinforced concrete, considering cracking, the nonlinear stress-strain behavior under short-time loadings, and the bond-slip interaction at the steel-concrete interface.

The finite difference technique has been satisfactorily applied to analyse plates in flexure. Example of this is the work done by A. K. Bhaumik and J. T. Hauley[4]. However, their analysis is applicable to metallic plates only.

In the present paper the finite difference method is used to establish the procedure which enables to take account of high discontinuity in reinforced concrete beams and plates. The analysis can be used to predict the full range behavior of reinforced concrete beams and reinforced concrete simply supported plate. Finally, by comparing the analytical results with test results and ACI (1971) recommendations[6], the accuracy of this method is checked.

2. GOVERNING EQUATIONS

(1) Assumptions

The mathematical formulation idealizing the behavior of reinforced concrete slab is based on the following simplifying assumptions:

(1) A point on a line which is normal to the undeformed neutral surface before bending remains on the line which is still normal to the deformed neutral surface.
(2) The normal stress σ_{zz} is small compared with the other stress components and may be neglected in the stress-strain relation.
(3) In bending, there are no strains in the neutral surface, (inextensibility of the neutral surface).
(4) Poisson's ratio effects are neglected ($\nu=0$).

(2) Sign Convention

In order to have a clear picture of the behavior of the system, the sign convention for the

* M. Eng., Graduate Student of Asian Institute of Technology.
** Member of JSCE, Associate Professor, Nihon University, former Associate Professor of AIT.
*** Member of JSCE, Associate Professor, Dept. of Civil Eng., Nagoya University, former Associate Professor of AIT.

forces and deformations is defined as follows:

Axes

The coordinate axes X and Y are designated in the plane of the plate and Z-axis perpendicular to the plane, as shown in **Fig. 1.** The deflection w measured along the Z axis of the plate is positive downwards.

Moments

Moments are considered positive when they produce compression on the upper surface of the plate and tension on the lower surface, as shown in **Fig. 1.**

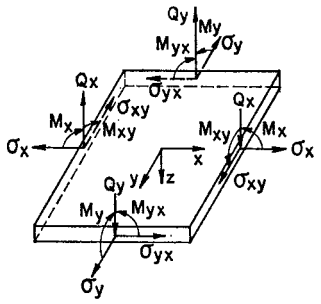

Fig. 1 Positive forces.

Stresses and Shear Forces

Stresses and shear forces are considered positive as shown in **Fig. 1.**

Torsional Moments

Torsional moments are considered positive if they are directed outward, as shown in **Fig. 1.**

(3) Governing Differential Equations

The governing equations of the plate taken from Timoshenko's textbook[18] are as follows:

Equilibrium Equations

$$\frac{\partial Q_x}{\partial X}+\frac{\partial Q_y}{\partial Y}+q=0$$

$$Q_y=\frac{\partial M_y}{\partial Y}+\frac{\partial M_{yx}}{\partial X}$$

$$Q_x=\frac{\partial M_x}{\partial X}+\frac{\partial M_{yx}}{\partial Y}$$

$$\therefore\quad \frac{\partial^2 M_x}{\partial X^2}+2\frac{\partial^2 M_{yx}}{\partial X\partial Y}+\frac{\partial^2 M_y}{\partial Y^2}+q=0$$

or

$$\frac{\partial^2 M_x}{\partial X^2}-2\frac{\partial^2 M_{xy}}{\partial X\partial Y}+\frac{\partial^2 M_y}{\partial Y}+q=0 \quad \cdots\cdots(1)$$

Curvature—Displacement Relationships

$$\phi_{xx}=\frac{\partial^2 w}{\partial X^2} \quad \cdots\cdots(2)$$

$$\phi_{yy}=\frac{\partial^2 w}{\partial Y^2} \quad \cdots\cdots(3)$$

$$\phi_{xy}=\frac{\partial^2 w}{\partial X\partial Y} \quad \cdots\cdots(4)$$

Moment—Curvature Relationships

for

$\nu=0$

$$M_x=-EI_x\phi_{xx} \quad \cdots\cdots(5)$$

$$M_y=-EI_y\phi_{yy} \quad \cdots\cdots(6)$$

$$M_{xy}=R\phi_{xy} \quad \cdots\cdots(7)$$

Thus, there are 7 equations for 7 independent variables, M_x, M_y, $M_{xy}(=-M_{yx})$, ϕ_{xx}, ϕ_{yy}, ϕ_{xy} and w.

For beam problem $M_y=0$, $M_{xy}=0$ in Eq. (1), then, the governing equation of beam is:

$$\frac{\partial^2 M_x}{\partial X^2}+q=0 \quad \cdots\cdots(8)$$

(4) Mathematical Formulation of Differential Equations by Finite Difference Method

The application of finite difference method to beam and plate under bending consists of rewriting the differential equations, Eqs. (1)~(4), in terms of unknown values of w, ϕ_{xx}, ϕ_{yy} and ϕ_{xy} at a finite number of nodal points. The method results directly in the formulation of a set of simultaneous linear algebraic equations for each nodal point.

The appropriate expression of differential equation using finite difference method can be easily found in many mathematics books. There are different methods of deriving the finite difference equation. Here the most common one is adopted.

Referring to **Fig. 2,** in which w is a function of x and y, the first finite difference approximation at (i, j) is

$$\left.\frac{dw}{dX}\right|_{i,j}=\frac{1}{2a}(w_{i+1,j}-w_{i-1,j})$$

the second derivative at (i, j) is

$$\left.\frac{\partial^2 w}{\partial X^2}\right|_{i,j}=\frac{1}{a^2}(w_{i+1,j}-2w_{i,j}+w_{i-1,j})$$

the first mixed partial derivative at (i, j) is

$$\left.\frac{\partial^2 w}{\partial X\partial Y}\right|_{i,j}=\frac{1}{4a^2}[w_{i+1,\,j+1}+w_{i-1,\,j-1}-w_{i+1,\,j-1}-w_{i-1,\,j+1}]$$

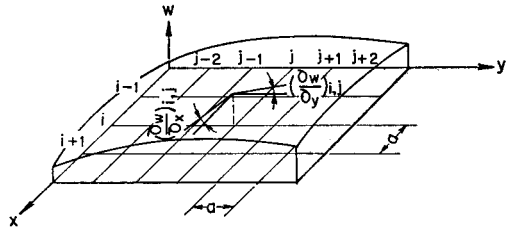

Fig. 2 Finite difference grid.

3. STRESS-STRAIN RELATIONS

The developed method is applicable to the

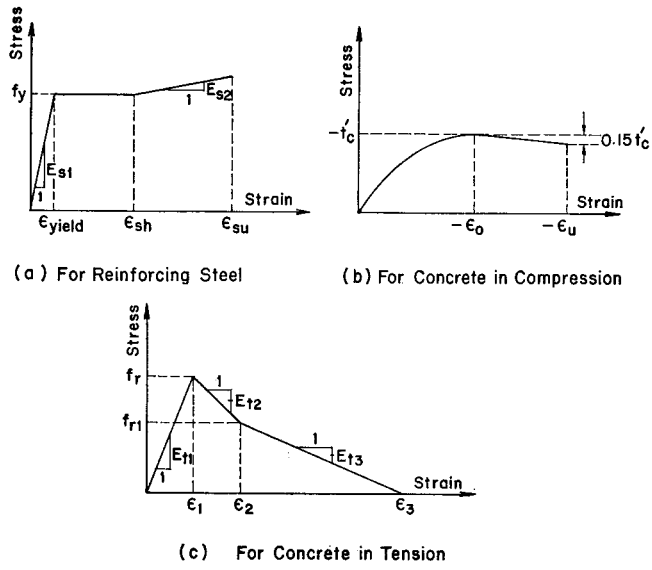

Fig. 3 Idealized stress-strain relationships.

materials of any stress-strain relationship. The behaviors of the reinforcing steel and the concrete at all stages of loading up to ultimate are represented by idealized stress-strain relationships and are expressed by a set of equations. Tensile stress and the corresponding strain are considered positive.

Reinforcing Steel

The tri-linear stress-strain curve in **Fig. 3**(a) is used. The variables required to define the curve are the yield stress f_y, the slopes E_{s1} and E_{s2}, and the strain ϵ_{sh} and ϵ_{su}, corresponding to the start of strain hardening and ultimate strength. Let ϵ_s be the strain of steel under loading.

$$F_1(\epsilon_s)=E_{s1}\cdot\epsilon_s \quad \text{for} \quad 0\leq\epsilon_s\leq\epsilon_{yield} \cdots\cdots(9)$$

$$F_2(\epsilon_s)=E_{s1}\cdot\epsilon_{yield}, \quad \epsilon_{yield}\leq\epsilon_s\leq\epsilon_{sh} \cdots\cdots(10)$$

$$F_3(\epsilon_s)=E_{s1}\cdot\epsilon_{yield}+E_{s2}(\epsilon_s-\epsilon_{sh}), \quad \epsilon_{sh}\leq\epsilon_s\leq\epsilon_{sn} \cdots\cdots(11)$$

Concrete in Compression

The empirical stress-strain relationship for concrete in compression proposed by Hognestad[10] is adopted here. It consists of a second-order parabola up to strain ϵ_0, corresponding to the compressive strength f_c', and a linear variation along a descending branch up to the ultimate strain level ϵ_u. This is a modification to Hognestad's idealization, with the maximum value of concrete stress being taken as f_c' rather than $0.85\ f_c'$[1]. Let ϵ_c be the strain of concrete in compression under loading and then the stress strain relations of the concrete in compression shown in **Fig. 3**(b) are derived as follows:

$$F_4(\epsilon_c)=f_c'\left(\frac{2}{\epsilon_0}-\frac{\epsilon_c}{\epsilon_0^2}\right)\epsilon_c \qquad 0\geq\epsilon_c\geq\epsilon_0 \cdots(12)$$

$$F_5(\epsilon_c)=f_c'\left(1-0.15\frac{\epsilon_c-\epsilon_0}{\epsilon_u-\epsilon_0}\right) \qquad \epsilon_0\geq\epsilon_c\geq\epsilon_u \cdots(13)$$

Concrete in Tension

The stress-strain relationship for concrete in tension is generally assumed linear up to the rupture modulus, then dropping abruptly to zero stress. This represents the behavior of the concrete at a section in which a crack will form. However, even after cracking, the concrete is still capable of resisting tensile forces in the parts between cracks. This has the effect of increasing the average stiffness of a slab within a given finite length compared to the stiffness of a section at which a crack is formed. This overall stiffening effect can be simulated by using a stress-strain relationship for concrete in tension which includes a descending branch to account for the effect of progressive cracking and the corresponding decrease of tension in the concrete between the cracks; the concept used by Scanlon and Murray[17]. The graph in **Fig. 3**(c) with a descending branch is therefore adopted in the analysis. The shape of the descending branch is based on experimental work of Evans and Marathe[9] and the author adopts it from A. Vebo and A. Ghali's study[1]. It consists of three strain levels ϵ_1, ϵ_2 and ϵ_3, three linear slopes E_{t1}, E_{t2} and E_{t3}. Let ϵ_t be strain of concrete in tension.

$$F_6(\epsilon_t)=E_{t1}\cdot\epsilon_t \qquad 0\leq\epsilon_t\leq\epsilon_1 \cdots\cdots(14)$$

$$F_7(\epsilon_t)=E_{t1}\epsilon_1+E_{t2}(\epsilon_t-\epsilon_1) \qquad \epsilon_1\leq\epsilon_t\leq\epsilon_2 \cdots\cdots(15)$$

$$F_8(\epsilon_t)=F_7(\epsilon_2)+E_{t3}(\epsilon_t-\epsilon_2) \qquad \epsilon_2\leq\epsilon_t\leq\epsilon_3 \cdots\cdots(16)$$

The choice of the parameters defining the eight F functions depends on the properties of steel and concrete. Values used in the analysis are given as input data of the grogram.

4. FLEXURAL AND TORSIONAL RIGIDITY OF CRACKED OR UNCRACKED REINFORCED CONCRETE REGION

(1) Flexural Rigidity of Reinforced Concrete Region

The determination of the rigidity of a cracked concrete region is difficult, because the cracks are distributed discontinuously. Furthermore the effect of tension stiffening, which plays an important role in overall rigidity of the cracked concrete region, reduces as the cracks increase.

Many methods have been proposed for dealing with this problem. A summary was given in a report by ACI committee 435[5]. The present paper does not attempt to define flexural rigidity EI directly. Instead, equilibrium equations, Eqs. (17) and (18), are used to find moment M. Then $EI=M/\text{curvature}$ is used in the analysis. Under certain loading condition the value of EI keeps on changing at every nodal point until it approaches to the exact value. The practical procedure of this approach is explained in **Appendix A**.

It is assumed that the reinforcing steel is subjected to uniaxial stress only. The stresses normal to the X—Z and Y—Z planes must make couples M_y and M_x respectively, and the sum of the stresses in the horizontal direction is zero. Therefore equilibrium Eqs. (17) and (18) can be expressed as follows:

$$\left.\begin{aligned}&\sum_{i=1}^{4} F_{sxi}+\frac{1}{\phi_{xx}}\int_{\varepsilon_{bx}}^{\varepsilon_{tx}} F_c(\varepsilon)d\varepsilon=0\\ \text{or}\quad&\sum_{i=1}^{4} F_{syi}+\frac{1}{\phi_{yy}}\int_{\varepsilon_{by}}^{\varepsilon_{ty}} F_c(\varepsilon)d\varepsilon=0\end{aligned}\right\}\quad\cdots\cdots(17)$$

$$\left.\begin{aligned}M_x=&\frac{1}{\phi_{xx}}\sum_{i=1}^{4} F_{sxi}(\varepsilon_{xi}-\varepsilon_{x1})\\&+\frac{1}{\phi_{xx}^2}\int_{\varepsilon_{bx}}^{\varepsilon_{tx}} F_c(\varepsilon)(\varepsilon-\varepsilon_{x1})d\varepsilon\\ M_y=&\frac{1}{\phi_{yy}}\sum_{i=1}^{4} F_{syi}(\varepsilon_{yi}-\varepsilon_{y1})\\&+\frac{1}{\phi_{yy}^2}\int_{\varepsilon_{by}}^{\varepsilon_{ty}} F_c(\varepsilon)(\varepsilon-\varepsilon_{y1})d\varepsilon\end{aligned}\right\}\quad\cdots\cdots(18)$$

in which ε_{xi} is the strain at the level of the ith steel layer normal to the Y—Z plane and F_{sxi} is the stress of the ith layer of steel in the X direction. The symbols are explained in **Fig. 4**.

(2) Torsional Rigidity of Reinforced Concrete Region

For beam problem, torsional rigidity of reinforced concrete sections before cracking can be calculated by St.-Venant's theory with reasonable accuracy[11], and the one after cracking can be derived successfully be Hsu's method[12]. However, it is still very difficult to evaluate the rigidity of the cracked concrete slab.

In this paper, the author tries to use layered model to derive an expression for torsional rigidity. For simplicity, the effects of reinforcing steel and the portion of concrete in tension are neglected.

For the plate problem, the element is divided into n layers as shown in **Fig. 5**. Under loading, each layer will deform as shown in **Fig. 6** and

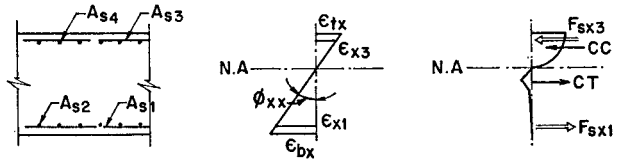

Fig. 4 Distribution of strains, stresses and forces in a slab-element.

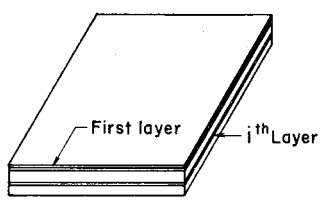

Fig. 5 Layered model of a slab element.

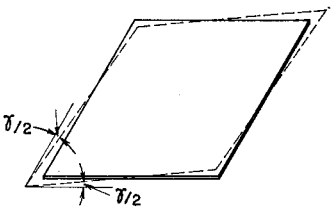

Fig. 6 Deformation of ith layer.

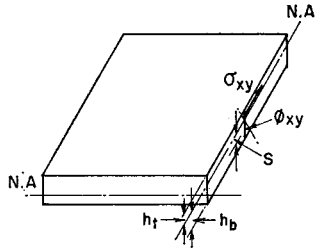

Fig. 7 A slab element under torsion.

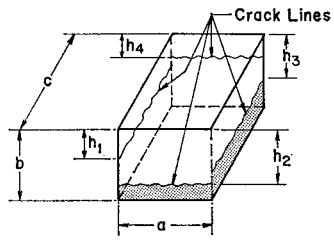

Fig. 8 A slab element under cracking.

$$\gamma=\frac{\sigma_{xy}}{G}=2\epsilon_{xy}$$

before cracking

for a plate element as shown in **Fig. 7**

$$\because\quad \epsilon_{xy}=\frac{1}{2G}\sigma_{xy} \text{ and } \epsilon_{xy}=-S\frac{\partial^2 w}{\partial X\partial Y}=-S\phi_{xy}$$

$$\therefore\quad M_{xy}=-\int_{-h_t}^{0} S\sigma_{xy}dS=-\int_{-h_t}^{0} S2G\epsilon_{xy}dS$$

$$=-\int_{-h_t}^{0} S2G(-S\phi_{xy})dS$$

$$=2G\phi_{xy}\int_{0}^{h_t} S^2dS=R\phi_{xy}$$

so the torsional rigidity before cracking is defined as:

$$R=2G\int_{0}^{h_t} S^2dS=\frac{2Gh_t^3}{3} \qquad \cdots\cdots(19)$$

in which h_t is the distance between the neutral axis and the top fiber of a section.

after cracking

After cracking, not all of the layers but only the layers and part of the layers within uncracked part of concrete can resist torsion. In other words, only the volume of the uncracked part of concrete, see **Fig. 8**, resist torsion after cracking. With this consideration the torsional rigidity R_{cr} is defined as follows: if R is the torsional rigidity before cracking and $h_{ij}(i, j=1 \text{ to } 4)$ is the smaller value of h_i and h_j, as shown in **Fig. 8**, then

$$R_{cr}=R\frac{h_{12}+h_{23}+h_{34}+h_{41}}{4b} \qquad \cdots\cdots(20)$$

5. PROCEDURE FOR NONLINEAR ANALYSIS

The cracking of the concrete under low tensile stress may be the dominating cause of the nonlinear behavior of reinforced concrete structures. Instead of taking account of individual cracks as they occur under loading, the effect of cracking is treated in average by changing the flexural rigidity EI, of the cracked elements. Other material nonlinearity effects are treated in a similar manner.

The numerical procedure starts with dividing the load into a finite number of increments and obtaining the stress-strain relations of concrete and steel from experiments. For each load increment, iterations are performed until the equilibrium and constitutive relations are satisfied within a certain allowable limit.

The analysis starts from the first loading increment and the major steps are as follows:

(1) to discretize the structure into several elements

(2) to formulate equations (1)~(4), or (2) and (8) for a beam problem, at every nodal point by finite difference technique as shown in section 2-4.

(3) to assemble all the equations

(4) to assume values for flexural rigidity EI and torsional rigidity R in the simultaneous equations of step (3)

(5) to solve for w, ϕ_{xx}, ϕ_{yy}, ϕ_{xy} at every nodal point

(6) to substitute curvature ϕ_{xx} and ϕ_{yy} at every nodal point into Eq. (17) to find the neutral axes NA

(7) to find moments M_x and M_y at every nodal point by Eq. (18)

(8) to modify R by Eq. (19) or (20)

(9) to compare $(EI_x)_1=M_x/\phi_{xx}$ and $(EI_y)_1=M_y/\phi_{yy}$ at every nodal point with the previous ones of step (4)

(10) if the differences in step (9) is within allowable limit then regard the values of w, ϕ_{xx}, ϕ_{yy} and ϕ_{xy} at every nodal points as being acceptable and go to step (11), otherwise, use the last EI and R values and go to step (5).

(11) to increase the load by a increment and go to steps (5) with the last EI and R values.

The process from step (4) to step (10) is to find the exact EI values. This approach is explained in **Appendix A**.

6. NUMERICAL EXAMPLES AND THEIR COMPARISON WITH EXPERIMENTAL RESULTS

To demonstrate the capability of the method

for analysing reinforced concrete members the following 4 examples are performed.

In these numerical analysis following input data were adopted; $\epsilon_0=0.002$, $\epsilon_u=0.0035$, $E_{t2}=E_{t3}$, $\epsilon_1=0.0001305$, $\epsilon_3=0.0009135$ for concrete (**Fig. 3**(b), (c)), $E_{s2}=0$ for steel (**Fig. 3**(a)).

(1) A beam 190 mm wide by 229 mm deep, a span of 3 047 mm and 1.77% reinforcing steel, tested by Alami and Ferguson[2], see **Fig. 9**.

(2) A beam 142 mm wide by 217 mm deep, a span of 3 420 mm and 1% reinforcing steel, tested by the Instituto de Materials Y Modelos Estructurales (IMME) at the Universidad Central de Venezuela Caracas, Venezuela Caracas, Venezuela and the Laboratory for Structural Models at MIT, from Angel L. Lazaro, III and Rowland Richards, Jr.[3], see **Fig. 10**.

(3) A beam 48 mm wide by 72 mm deep, a span of 1 128 mm and 1% reinforcing steel, tested by IMME, same as example (2), see **Fig. 11**.

For the above three examples the comparisons made include the center deflections of the beams by (a) experiment (b) analytical results proposed by the author (c) analytical results proposed by Angel L[3] and (d) ACI 1971 recommendation[6].

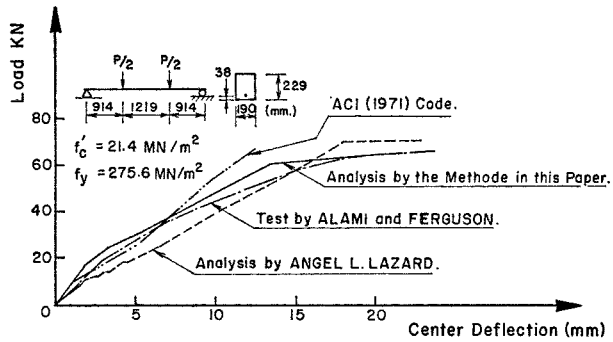

Fig. 9 Load-deflection curves for the test by Alami and Ferguson.

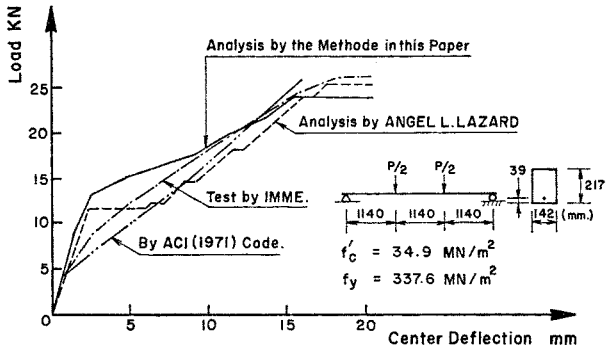

Fig. 10 Load-deflection curves for the beam $142\times217\times3\,420$ mm tested by IMME.

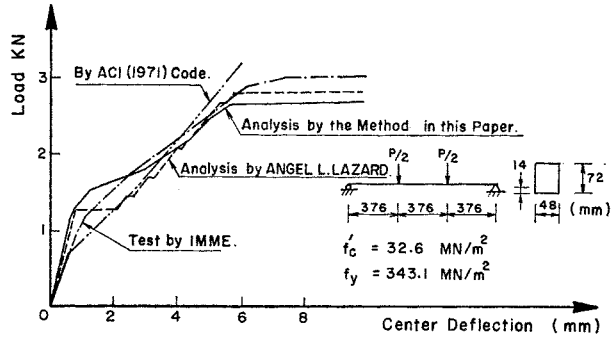

Fig. 11 Load-deflection curves for the beam $48\times72\times1\,128$ mm tested by IMME.

The compared results are shown in **Fig. 9** to **Fig. 11**. The agreement between analytical results proposed in this paper and test results is better than that shown by the results of Angel's[8]. They also have almost the same accuracy as the results obtained according to ACI code recommendations in approaching the experimental ones. But for example (1), with higher steel ratio $p=1.77\%$, the results obtained by ACI code recommendations fail to predict the behavior of that beam at higher loading.

Angel and Lagard's numerical results have different features in **Figs. 9** and **10**. They did not give any reasons for it but the different ratio of reinforcement might be its reason for the difference.

(4) A simply supported slab 3.048×3.048 m, 83 mm deep, 0.0259 cm^2/cm reinforcing steel area in X and Y directions, uniformly loaded, tested by M. A. Muspratt[15] see **Fig. 12** and **Fig. 13**.

The slab is divided into 16, 36 and 64 elements and the results in each case are compared with test results. The calculated results with 36 and 64 elements show better loading capacity because they include more terms in the simultaneous equations which means the effects of moments and torsions are included more completely. For the cases of 36 and 64 elements the results are almost the same in the small deflection region (within 5 cm of deflection) although the later shows better agreement with the test results; assuring a convergence criterion as the size of the discrete element is reduced. If we neglect the effect of torsion by excluding all the torsional terms in the simultaneous equations, the deflections obtained are the same before the yielding of steel develops as those cases in which torsional effect is considered. It seems that torsion has no significant effect on the deflection of slabs in elastic range and it will increase the loading capacity. Moreover the ultimate load obtained by excluding the torsional effect in the analysis approaches the ultimate load obtained by yield-line theory[7]. This phenomenon is reasonable because the ultimate load in the yield-line theory is derived by the ultimate moment capacities in two orthogonal directions (X and Y directions) only.

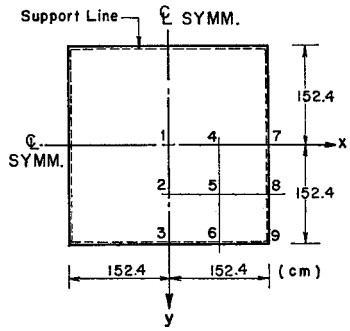

Fig. 12 Simply supported two-way slab (16 elements).

In the numerical work, the flexural or torsional rigidity were supposed to be converged when a ratio of the difference between (i-1)th step and ith step to the rigidity at (i-1)th step is less than 0.001.

As for numbers of the iteration, around twenty iterations were required under the loads which gave yielding of reinforcement, however around six iterations were sufficient in the elastic range.

There are fairly large discrepancies between the experiments and the authors' numerical results in craking range in **Figs. 10** and **11**. This kind of discrepancy is not detected for the slab in **Fig. 13**. Concrete characteristic in tension is assumed in **Fig. 3**(c) which shows that concrete keeps tension strength after crack. The cracks may easily cross a whole width of a section in a beam, but they are confined to a certain area on the surface of a slab. Therefore the evalua-

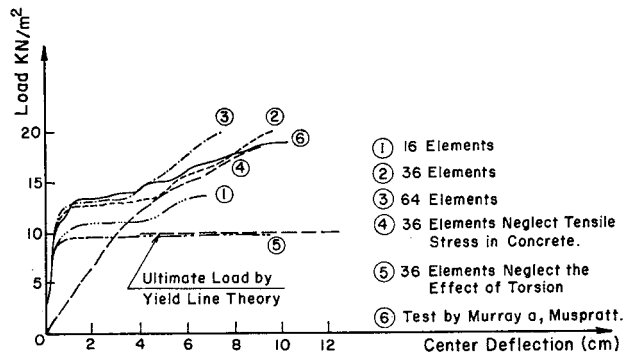

Fig. 13 Load-deflection curves for the slab tested by Muspratt.

tion of concrete tension strength in **Fig. 3**(c) is more reasonable in slabs than in beams. A trial numerical works reveal that zero-strength after rupture modulus gives better results in beam analysis.

7. CONCLUSIONS

The main purpose of this paper is to present a method for the determination of the complete load—deflection behavior of simply—supported slabs subjected to uniformly distributed load. Upon investigation, the following conclusions can be derived.

(1) The results of this method used to represent the behavior of reinforced concrete beams and plate are satisfactory.

(2) The method is able to predict the entire sequence of behavior under increasing transverse loading from first cracking to yielding of the reinforcing steel. Any arbitrary variation in the materials can be admitted.

(3) It is found that the tension stiffening effect has a very significant influence on the post-cracking response of concrete slabs but not on the behavior at the ultimate stage.

(4) Torsion has no significant influence on the deflection of reinforced concrete plate under uniform load in the elastic region, but it will increase the load carrying capacity of slab.

(5) The small deflection theory is used to arrive at the analytical behavior. Discrepancy in large deflection range comes from neglecting the effect of large deflection and unaccurate material nonlinearity. When the deflection exceeds 5 cm, in the case of example (4), the analytical results do not approach well to the test result, but it is not important in the practical usage because the maximum allowable deflection recommended by ACI (1971) code[6] for all two-way construction is $l/180$, which is 1.69 cm in example (4), much smaller than 5 cm.

Applicability of the proposed method is not examined in this paper for other loading cases such as concentrated load or non-uniform load, or other supporting conditions like clamped slabs. The authors' study of uniformly loaded simple slab suggests however that the adopted method may be applicable to other cases, though the accuracy is not so good because the finite difference analysis is itself not highly accurate for non-uniform loading or complicated supporting condition even in the elastic range.

In this paper an engineering simple evaluation is successfully proposed, however the rigorous evaluation of torsional rigidity of slabs gives another ploblem.

APPENDIX A

The iterative process from step (4) to (10) in Chapter 5 can be explained as follows:

Referring to **Fig. A**(1) which is a real moment—curvature relation diagram.

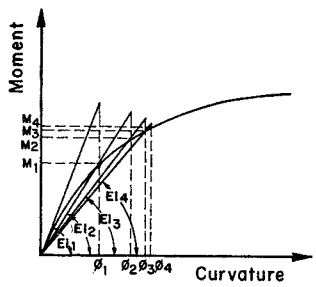

Fig. A(1) Diterative process.

(a) from step (4) we assume flexural rigidity EI_1.
(b) from step (5) we obtain corresponding curvature ϕ_1.
(c) from step (6) and step (7) we obtain corresponding Moment M_1
(d) in step (8) compare $EI_2=M_1/\phi_1$ with EI_1
(e) if the difference between EI_1 and EI_2 is not within allowable limit Q then substitute EI_2 into step (5) and repeat the procedure until $(EI)_n-(EI)_{n-1}$ is within allowable value.

APPENDIX B

Example of simultaneous equations for the case of simply supported plate with 16 elements, see **Fig. 12**.

REFERENCES

1) Ake Vebo and Amin Ghali: Moment Curvature Relation of Reinforced Concrete Slabs, Journal of the Structural Division, ASCE, Vol. 103, No. ST3, Pro. paper 12778, pp. 515~531, March 1977.
2) Alami, Z. Y. and P. M. Ferguson: Accuracy of Models Used in Research on Reinforced Concrete, Journal of the American Concrete Institute, Vol. 60, No. 11, pp. 1643~1663, Nov. 1963.
3) Lazaro, A. L., III and Rowland Richards, Jr.: Full-Range Analysis of Concrete Frames, Journal of the Structural Division, ASCE, Vol. 99, No. ST8, Pro. paper 9934, pp. 1761~1783, Aug. 1973.
4) Bhaumik, A. K. and John T. Hanley: Elasto—Plastic Plate Analysis by Finite Differences, Journal of the Structural Division, ASCE, Vol.

				$-2EI$			$2EI$	$-2EI$	$2EI$							w_1	qa^2
					$-2EI$	$2EI$		EI	$-2EI$							w_2	qa^2
					EI	$-2EI$				$-2EI$	EI			R		w_5	qa^2
				EI			$-2EI$			$2EI$	$-2EI$					w_4	qa^2
-2			2	$-a^2$												ϕ_{x1}	0
	-2	2			$-a^2$											ϕ_{x2}	0
	1	-2				$-a^2$										ϕ_{x5}	0
1			-2				$-a^2$									ϕ_{x4}	0
-2	2							$-a^2$								ϕ_{y1}	0
1	-2								$-a^2$							ϕ_{y2}	0
		-2	1							$-a^2$						ϕ_{y5}	0
		2	-2								$-a^2$					ϕ_{y4}	0
0.25												$-a^2$				ϕ_{xy5}	0
	0.5												$-a^2$			ϕ_{xy6}	0
		1												$-a^2$		ϕ_{xy9}	0
			0.5												$-a^2$	ϕ_{xy8}	0

$$\begin{bmatrix} 0 & A^* \\ \hline B & C \end{bmatrix}\begin{bmatrix} S_1 \\ \hline S_2 \end{bmatrix}=\begin{bmatrix} R_1 \\ \hline 0 \end{bmatrix} \qquad \begin{aligned} S_1&=-(AC^{-1}B)^{-1}R_1 \\ S_2&=-C^{-1}BS_1 \end{aligned}$$

* The EI values in matrix A are different by column, for example, the EI values in the first column of matrix A mean EI_{x1} and the EI values in the second columns mean EI_{x2} etc.

93, No. ST5, Pro. paper 5511, pp. 279~293, Oct. 1967.

5) American Concrete Institute Committee 435: Deflection of Reinforced Concrete Flexural Members, Journal of the American Concrete Institute, Vol. 63, No. 6, pp. 637~673, June 1966.

6) American Concrete Institute Standard 318-71: Building Code Requirements for Reinforced Concrete, Detroit, Mich. pp. 27~28, 1971.

7) Chu-Kia Wang and Charles G. Salmon: Reinforced Concrete Design, Second Edition, International Textbook Company, pp. 735~774.

8) Chung-Hyun Nam and Charles G. Salmon: Finite Element Analysis of Concrete Beams, Journal of the Structural Division, ASCE, Vol. 100, No. ST12, Pro. paper 11016, pp. 2419~2431, Dec. 1974.

9) Evans, R. H. and M. S. Marathe: Microcracking and Stress-Strain Curves for Concrete in Tension, Materiaux et Constructions, Vol. 1, pp. 61~68, Jan.–Feb., 1968.

10) Hognestad, E.: A Study of Combined Bending and Axial Load in Reinforced Concrete Members, Engineering Experimental Station Bulletin No. 399, University of Illinois, Urbana, Ill., p. 128, 1951.

11) Hsu, Thomas T. C.: Torsion of Structural Concrete—Behavior of Reinforced Concrete Rectangular Members, Torsion of Structural Concrete, SP-18, American Concrete Institute, Detroit, pp. 261~306, 1968.

12) Hsu, Thomas T. C.: Post-Cracking Torsional Rigidity of Reinforced Concrete Sections, Journal of American Concrete Institute, No. 70-40, pp. 352~360, May 1973.

13) Jofriet, J. C. and Gregory M. McNeice: Finite Element Analysis of Reinforced Concrete Slabs, Journal of the Structural Division, ASCE, Vol. 97, No. ST3, pp. 785~805, March 1971.

14) Wanchoo, M. K. and Gerald W. May: Cracking Analysis of Reinforced Concrete Plates, Journal of the Structural Division ASCE, Vol. 101, No. ST1, Proc. paper 11059, pp. 201~215, Jan. 1975.

15) Muspratt, M. A.: Behavior of Simply Supported Slabs, Journal of the Structural Division, ASCE, Vol. 95, No. ST12. Proc. paper 6945, pp. 2703~2721, Dec. 1969.

16) Ngo and Scordelis: Finite Element Analysis of Reinforced Concrete Beams, Journal of American Concrete Institute, Proceedings, Vol. 64, No. 3, pp. 152~163, March 1967.

17) Scanlon, A. and Murray D. W.: An Analysis to Determine the Effects of Cracking in Reinforced Concrete Slabs, Proceedings of the Specialty Conference on Finite Element Method in Civil Engineering, Montreal, Canada, pp. 841~868, June 1 and 2, 1972.

18) Timoshenko and Woinowsky-Krieger: Theory of Plate and Shells, Second Edition, McGraw Hill Kogakusha, Ltd. pp. 80~81.

(Received September 11, 1980)